International Journal of Automation and Computing 14(3), June 2017, 321-339
DOI: 10.1007/s11633-017-1061-3

Multi-objective Invasive Weed Optimization of the LQR Controller

Hafizul Azizi Ismail[1, 2] Michael S. Packianather[1] Roger I. Grosvenor[1]

[1]School of Engineering, Cardiff University, Queen's Buildings, The Parade, Cardiff CF24 3AA, UK

[2]German Malaysian Institute, Jalan Ilmiah, Taman Universiti, Kajang 43000, Selangor, Malaysia

Abstract: The Robogymnast is a triple link underactuated pendulum that mimics a human gymnast hanging from a horizontal bar. In this paper, two multi-objective optimization methods are developed using invasive weed optimization (IWO). The first method is the weighted criteria method IWO (WCMIWO) and the second method is the fuzzy logic IWO hybrid (FLIWOH). The two optimization methods were used to investigate the optimum diagonal values for the Q matrix of the linear quadratic regulator (LQR) controller that can balance the Robogymnast in an upright configuration. Two LQR controllers were first developed using the parameters obtained from the two optimization methods. The same process was then repeated, but this time with disturbance applied to the Robogymnast states to develop another set of two LQR controllers. The response of the controllers was then tested in different scenarios using simulation and their performance evaluated. The results show that all four controllers are able to balance the Robogymnast with varying accuracies. It has also been observed that the controllers trained with disturbance achieve faster settling time.

Keywords: Pendulum, multi-objective optimization, linear quadratic regulator (LQR), robogymnast, underactuated robots.

1 Introduction

Underactuated mechanism is a system whose number of control inputs is less than the dimension of the configuration space. Control of underactuated mechanism is one of the major research topics in control engineering and robotics[1]. The ability to control underactuated mechanism through the manipulation of its natural dynamics will allow for the design of more energy efficient machines with the ability to achieve smooth motion comparable to that found in the natural world. The multilink pendulum is a popular example of an underactuated mechanism. Its simplicity and versatility makes it an attractive test bed for underactuated mechanism control design[2]. Pendulums are excellently suited to illustrate hybrid systems and control of chaotic systems[3]. Numerous studies have been conducted on stabilizing an inverted pendulum[4−7]. Multi-objective optimization (MOO) has become an important part of optimization activities. Many real-world optimization problems are naturally posed as nonlinear programming problems having multiple conflicting objectives. A multi-objective optimization problem deals with more than one objective function[8]. Li et al.[9] designed an approach of weighting matrices for linear quadratic regulator (LQR) based on multi-objective evolutionary algorithm. The algorithm uses J function and pole placement as the objective function. Simulation results show that shorter settling time and smaller amplitude value deviating from steady-state are achieved using the proposed approach. An optimal design of LQR weighting matrices based on intelligent optimization methods such as genetic algorithm (GA), particle swarm optimization (PSO), differential evolution (DE) and imperialist competitive algorithm (ICA) to solve optimization problem of LQR for a robot manipulator was done in [10]. A comparison of all results was done by combining criteria like speed of response, the close-loop pole locations, and maximum level of control effort into an objective function to find the best weighting matrices in the LQR controller. An optimal trade-off design for fractional order (FO)-PID controller is proposed with a linear quadratic regulator (LQR) based technique using two conflicting time domain objectives[11]. The research deals with problems such as choosing optimal weights and time delays in the LQR formulation. Reference [12] utilized the multi-objective invasive weed optimization (MOIWO) to design the impedance controller for a prosthesis test robot. The criteria for this optimization problem are the required amount of force and motion tracking. Simulation results showed that the solutions that were designed for motion tracking performed motion tracking perfectly but failed to reproduce the desired forces. While the solution that was designed for force tracking deviated from the desired motion in order to produce the desired force. An improved artificial bee colony (ABC) algorithm was developed by [13]. The improved ABC was then used to optimize the performance of the LQR controller for a circular-rail double pendulum system by minimizing the value of the cost function J. The improved ABC algorithm outperformed the traditional ABC algorithm in optimizing the parame-

Research Article
Manuscript received January 22, 2016; accepted July 19, 2016; published online March 17, 2017
Recommended by Associate Editor De Xu

ters of the LQR controller for inverted pendulum system. In previous investigations[14], the author applied both the cost function (J) and settling time (T) as separate fitness criteria. Settling time (T) is the time taken for the Robogymnast to achieve an upright stable postion. The investigations show that using J as the fitness criterion leads to the design of an upright balancing LQR controller that is more efficient in terms of power but with slower reaction time. Using T as the fitness criterion leads to the design of a LQR controller that has faster reaction time but is less efficient in terms of power. In this research a hybrid J and T fitness criteria is proposed to get the best of both controllers. To incorporate the two fitness criteria simultaneously, two novel MOO techniques are proposed in the design of the LQR controller for upright balancing of triple link pendulum.

In this paper, the diagonal values of the LQR Q matrix are selected using modified invasive weed optimization (IWO) algorithms. The first technique is the weighted criteria method IWO (WCMIWO) which combines the values of cost function (J) and settling time (T) into a single fitness criterion with the help of weights. The second technique is the fuzzy logic IWO hybrid (FLIWOH) which analyses the values of J and T. These two values are then evaluated and assigned a membership value which will then be used as the fitness criterion. The performance of the two techniques are then compared and analyzed. The performance of the resulting controllers will also be analyzed with and without disturbance applied to the system. The criteria that will be used to evaluate the controllers are the settling time, input voltages, the maximum angular deflection it can recover from and ability to remain upright with disturbance applied to the system. The paper is organized as follows. First a description of the Robogymnast system is explained. Next a brief introduction to LQR is given. In the multi-objective optimization (MOO) section the various types of MOO methods are briefly discussed. Next an explanation on IWO is given and followed by its application in LQR controller design. The following section describes the WCMIWO and its results. This is followed by the description of the FLIWOH and its results. In Section 9, the previous methods are repeated with disturbance applied to the system. A discussion of the findings and results is provided in the next section. Finally, a summary of the paper is provided.

2 System description

The triple link under-actuated mechanism (Robogymnast) is depicted in Fig. 1[15]. The frame of the Robogymnast is made from 50 mm diameter carbon fibre tubes weighing 0.213 kg/m. Aluminium components are attached to the ends of each link to provide the structures for mounting sensors and actuators. Physical parameters of the system are designed according to the features of a human gymnast swinging on a freely rotating high bar with his hands firmly fixed to the bar. Each link represents a body part or a group of body parts on a human. Link 1 represents the arms (without elbows and wrists). Link 2 represents the head and torso. Link 3 represents the legs (without knees and ankles). Joint 1 (hands) consists of a steel shaft mounted of ball bearings with a potentiometer mounted to measure angle of rotation of Link 1. Joints 2 (shoulders) and 3 (hip) are split into two sections. The first section is similar to joint 1 with a potentiometer to measure the relative angle of each link. The second section is the output shaft of the drive unit (direct current (DC) motor/gearbox). The Robogymnast is controlled by a PC equipped with appropriated analog to digital (AD)/digital to analog (DA) converters. C++ programmes are used to transmit the input/output commands between the PC and Robogymnast[7].

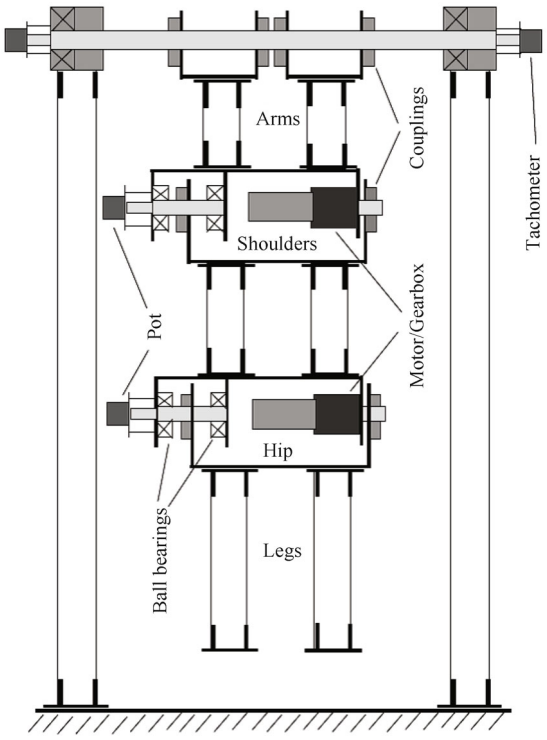

Fig. 1 Robogymnast system diagram

3 Linear quadratic regulator

The LQR is a well-known design technique that provides practical feedback gains. It is a multivariable controller as it can control displacement of the angles of the triple inverted at the same time[16]. Extensive research in the controls field has shown on multiple occasions that LQR is well suited for inverted pendulum stabilization[17]. The objective of LQR is to find the minimum value of the following cost function:

$$J = \int_0^\infty [x^{\mathrm{T}}(t)Qx(t) + u^{\mathrm{T}}(t)Ru(t)]\mathrm{d}t \tag{1}$$

where $u(t)$ is unconstrained, Q is required to be symmetric, positive semi definite matrix and R is required to be a symmetric positive definite matrix. For LQR the input will

be as the following:

$$u(t) = -Kx(t) \tag{2}$$

where K is the gain matrix required by the LQR. By applying (2) into the state space equation the following equation will emerge:

$$\dot{x} = (A - BK)x. \tag{3}$$

To obtain the value of K the following equation is then applied:

$$K = R^{-1}B^{\mathrm{T}}P. \tag{4}$$

Using the Algebraic Riccati Equation below the value of P can be obtained:

$$A^{\mathrm{T}}P + PA - PBR^{-1}B^{\mathrm{T}}P + Q = 0. \tag{5}$$

The value of K can then be obtained from (4). In order to implement a LQR controller, one must select suitable weighing matrices. For the Robogymnast, the value of Q will penalize the states while the value of R will penalize the inputs. For this reason, the elements of the Q matrix were selected to be much larger than the elements of the R matrix. In this paper, the settling time (T) is also selected as one of the fitness criteria along with cost function J. The objective of the MOO is to find a set of solutions with the minimum value of T and J.

4 Multi-objective optimization

Multi-objective optimization is the process of optimizing systematically and simultaneously a collection of objective functions. It originally grew out of three areas: economic equilibrium and welfare theories, game theory and pure mathematics[18]. Formally, MOO refers to simultaneous optimization (i.e., maximization and/or minimization) of two or more objective functions, which are often in conflict with one another. This optimization problem can be stated as follows[19]:

$$Optimize(f_1(x), f_2, \cdots, f_n). \tag{6}$$

Subject to

$$\begin{aligned} &g_i(x) \leq 0,\ i = 1, 2, \cdots, n_i \\ &h_i(x) = 0,\ i = 1, 2, \cdots, n_e \\ &x_1 = x = x_u \end{aligned} \tag{7}$$

where n is the number of objective functions to be simultaneously optimized, x is the vector of m decision variables (continuous and/or discontinuous) with lower (x_i) and upper (x_u) bounds, n_i and n_e are the number of inequality (g) and equality (h) constraints, respectively. The feasible space, F is the set of vectors x that satisfy all the constraints and bounds in (7). In contrast to the single-objective optimization case, where the optimal solution is clearly defined, in MOO problems there is a whole set of trade-offs giving rise to numerous Pareto optimal solutions[20].

4.1 Types of multi-objective optimization

The primary goal of MOO is to model a decision maker′s preference thus MOO methods are categorized depending on how the decision-maker articulates these preferences. MOO can be divided into three major categories[16]:

1) Methods with a priori articulation of preferences- Allow the user to specify preferences which may be articulated in terms of goals or relative importance of different objectives. Examples of this methods are:

a) Weighted global criterion method
b) Weighted sum method
c) Lexicographic method
d) Weighted min-max method
e) Exponential weighted criterion
f) Weighted product method
g) Goal programming methods
h) Bounded objective function method
i) Physical programming.

2) Methods for posteriori articulation of preference- Preferences are selected from a group of solutions through the use of an algorithm that is used to determine the representation of the generated Pareto optimal set. Examples of this methods are:

a) Physical programming
b) Normal boundary intersection (NBI) method
c) Normal constraint (NC) method.

3) Methods with no articulation of preferences- Do not require any articulation of preferences. Examples of this methods are:

a) Global criterion methods
b) Nash arbitration and objective product method
c) Raos method.

In this paper, two MOO methods with a priori articulation of preferences are utilized to search for the optimized parameters of the LQR controller for the Robogymnast. The first method is a weighted sum method and the second method is a combination of fuzzy logic and IWO.

5 Invasive weed optimization

Invasive weed optimization (IWO) was selected as the basis for the MOO techniques due to its simplicity and flexibility. IWO has some distinctive properties in comparison with traditional numerical search algorithm like reproduction, spatial dispersal and competitive exclusion[21]. A flowchart of IWO is shown in Fig. 2. Equation (8)[22] illustrates the spatial distribution equation of the IWO.

$$\sigma_{iter} = \frac{iter_{\max} - iter^n}{iter_{\max}{}^n}(\sigma_{initial} - \sigma_{final}) + \sigma_{final}$$

σ_{iter}= standard deviation at present step
$\sigma_{initial}$= initial standard deviation

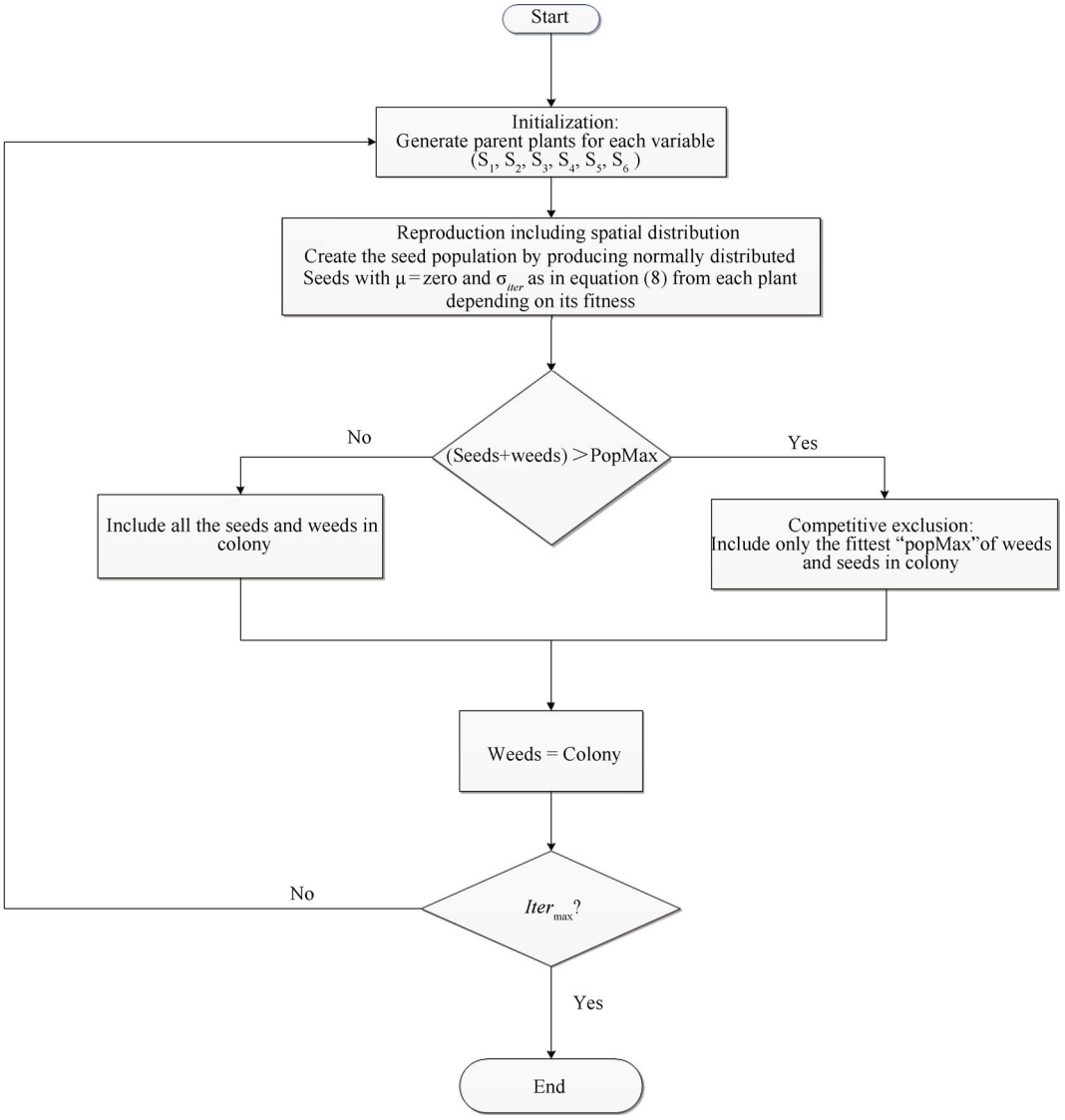

Fig. 2 Flowchart for invasive weed optimization algorithm[23]

σ_{final}= final standard deviation
$iter_{\max}$= maximum iteration
$iter$= current iteration
n= modulation index. (8)

6 Application of IWO in LQR controller design

The IWO is applied to find the global optimal solution of LQR controller in order to minimize the settling time and voltage required for the Robogymnast to go from an unbalance inverted configuration to a balanced upright configuration. The Q and R are set as diagonal matrices.

$$Q=\begin{bmatrix} Q_1 & 0 & 0 & 0 & 0 & 0 \\ 0 & Q_2 & 0 & 0 & 0 & 0 \\ 0 & 0 & Q_3 & 0 & 0 & 0 \\ 0 & 0 & 0 & Q_4 & 0 & 0 \\ 0 & 0 & 0 & 0 & Q_5 & 0 \\ 0 & 0 & 0 & 0 & 0 & Q_6 \end{bmatrix} \quad R=\begin{bmatrix} R1 & 0 \\ 0 & R2 \end{bmatrix}.$$

For the optimization process, parameters $R1$ and $R2$ of LQR controller are set to be at 1 and the values of Q are to be optimized. This is because for this application more importance is put on the control of the states rather than the inputs. In order to ensure that the Q matrix is a symmetric, positive semi definite matrix, Q is set as

$$Q = Q_{seeds} \times Q_{seeds}^{\mathrm{T}} \tag{9}$$

where Q_{seeds} is a diagonal matrix consisting of IWO seeds $(S_1, S_2, S_3, S_4, S_5, S_6)$ and Q_{seeds}^{T} is its transpose matrix.

$$Q_{seeds}=\begin{bmatrix} S_1 & 0 & 0 & 0 & 0 & 0 \\ 0 & S_2 & 0 & 0 & 0 & 0 \\ 0 & 0 & S_3 & 0 & 0 & 0 \\ 0 & 0 & 0 & S_4 & 0 & 0 \\ 0 & 0 & 0 & 0 & S_5 & 0 \\ 0 & 0 & 0 & 0 & 0 & S_6 \end{bmatrix}.$$

The optimization process is applied for an initial deflec-

tion of absolute angles $\theta_1 = 3^\circ$, $\theta_2 = 3^\circ$, $\theta_2 = 3^\circ$. These are the estimated maximum deflection angles the Robogymnast can make before the system becomes incapable of bringing it back to a balanced upright configuration. The objective of the controller is to obtain a relative angle of $q_1 \leq 0.001$ rad, $q_2 \leq 0.001$ rad and $q_3 \leq 0.001$ rad, where

$$q = \begin{bmatrix} q_1 \\ q_2 \\ q_3 \end{bmatrix} = \begin{bmatrix} \theta_1 \\ \theta_2 - \theta_1 \\ \theta_3 - \theta_2 \end{bmatrix}.$$

7 Weight criteria method invasive weed optimization

The weight criteria method invasive weed optimization (WCMIWO) technique uses both J and T in determining the fitness of each set of seeds. The fitness criteria JT is calculated as below

$$JT = (W_J \times J) + (W_T \times T) \tag{11}$$

where W_J and W_T are the multiplied weights of J and T respectively whose values are selected through trial and error. The weights are necessary due to J being significantly larger than T thus to ensure that J does not dominate the resulting fitness criterion JT. The set seeds are arranged in an ascending order with the smallest value of JT as the fittest set seeds.

A set seed is a combination of six seeds that make up S_1, S_2, S_3, S_4, S_5 and S_6. The number of maximum seed sets is 500. This is to ensure that the number of seeds is not too large so as not to slow down the search time. Maximum number of iterations is set as 10. Through trial and error, it is found that any larger number of iterations would not contribute to any improvement to the search process. The target angle is set at 0.001 rad which is close enough to be considered stable and inverted. To avoid local minima, different random search ranges were tried, starting with a search range $[0 - 10\,000]$ and moving on to smaller ranges. Due to (9), if the value of the seeds is too large it will result in exceedingly large Q matrix values. It was found that the search range $[0 - 1\,000]$ gives the best result. The initial standard deviation is selected as 50 and used in (8), as it is found to be suitable for initial spatial distribution for the given range $[0 - 1\,000]$. The final standard deviation is selected as 0.5 to ensure that the final set of seeds is not too widely dispersed from a potentially optimum set of plants. Table 1 shows the WCMIWO parameters used in the optimization process.

7.1 WCMIWO results

Table 2 shows the top ten best seed sets obtained from a population of 500. The minimum J value obtained is 100.183 and the fastest time is 6.35 s.

7.2 Simulation results of LQR on robogymnast

The fittest seeds, $S_1 = 50.348$, $S_2 = 500.587$, $S_3 = 400.658$, $S_4 = 250.002$, $S_5 = 150.174$ and $S_6 = 100.002$ are selected for analysis. Using (7), the Q matrix obtained from the seeds is

$$Q = \begin{bmatrix} 2.507 \times 10^5 & 0 & 0 & 0 & 0 & 0 \\ 0 & 2.506 \times 10^5 & 0 & 0 & 0 & 0 \\ 0 & 0 & 1.605 \times 10^5 & 0 & 0 & 0 \\ 0 & 0 & 0 & 0.625 \times 10^5 & 0 & 0 \\ 0 & 0 & 0 & 0 & 0.226 \times 10^5 & 0 \\ 0 & 0 & 0 & 0 & 0 & 0.1 \times 10^5 \end{bmatrix}$$

and the corresponding gain matrix is

$$K = \begin{bmatrix} -0.508 \times 10^3 & -0.217 \times 10^3 & -0.027 \times 10^3 \\ -0.427 \times 10^3 & -0.192 \times 10^3 & 0.007 \times 10^3 \\ 0.093 \times 10^3 & 0.049 \times 10^3 & 0.006 \times 10^3 \\ 0.079 \times 10^3 & 0.041 \times 10^3 & 0.005 \times 10^3 \end{bmatrix}.$$

Table 1 WCMIWO parameters

Variable	Value	Description
Number of initial plants	5	Number of randomly chosen values from the solution space
Minimum number of seeds	1	Minimum population of solutions
Maximum number of seeds	500	Maximum population of solutions
Initial value of standard deviation	50	Standard deviation used for spatial distribution of plants
Final value of standard deviation	0.5	Final standard deviation used for spatial distribution of plants
Maximum number of iterations	10	Number of iterations
Nonlinear Modulation Index	0.01	–
Weight of J	1E+6	Weightage of J
Weight of T	10	Weightage of T
Target angle	$q_1 \leq 0.001$ rad $q_2 \leq 0.001$ rad $q_3 \leq 0.001$ rad	The angle where time is recorded and used as the fitness criterion
Search range	$0 - 1\,000$	Search range used based on trial and error

Table 2 WCMIWO results

S_1	S_2	S_3	S_4	S_5	S_6	Time to reach the upright position (s)	J×10^5	JT
50.348	500.587	400.658	250.002	150.174	100.002	6.35	222.964	85.80
500.682	150.726	500.307	250.176	50.385	0.000	8.88	100.183	98.77
200.307	400.439	350.916	300.782	150.435	450.882	11.78	329.936	150.74
899.160	649.006	649.913	550.639	250.005	250.596	8.06	747.046	155.45
540.079	647.506	890.389	494.867	199.148	491.786	8.00	777.002	157.70
543.478	648.526	893.789	496.567	199.487	494.506	8.00	781.639	158.16
545.477	649.126	895.788	497.567	199.687	496.106	8.03	784.371	158.69
546.901	649.553	897.212	498.278	199.830	497.244	8.03	786.319	158.88
548.008	649.885	898.319	498.832	199.940	498.130	8.03	787.835	159.03
548.914	650.157	899.225	499.285	200.031	498.855	8.03	789.077	159.16

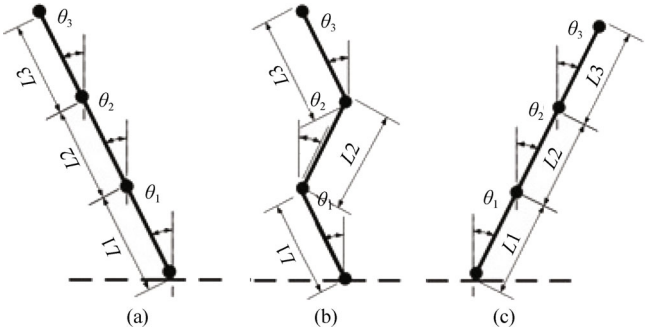

Fig. 3 Configurations of Robogymnast (a) $\theta_1 = -3°$, $\theta_2 = -3°$, $\theta_3 = -3°$, (b) $\theta_1 = -3°$, $\theta_2 = 3°$, $\theta_3 = -3°$, (c) $\theta_1 = 3°$, $\theta_2 = 3°$, $\theta_3 = 3°$

In order to verify the effectiveness of the WCMIWO algorithm, the parameters obtained are applied to a Matlab program created by the authors. The results are then compared for three different configurations as shown in Fig. 3 to ensure that the optimization can be implemented in various configurations.

Fig. 4 shows the system response and reveals that the voltages required to bring the Robogymnast to a stable upright position with the initial absolute angular position equal to [–3°, –3°, –3°] are 12 V for both motor 1 and motor 2. It can be seen that the time (T) taken to reach a stable upright position is 6.35 s.

Fig. 5 depicts the reaction of the Robogymnast as it attempts to stabilize itself from an initial absolute angular configuration equal to [–3°, 3°, –3°]. The maximum voltage (u_1) required by motor 1 is 6.62 V and motor 2 (u_2) is 1.55 V.

Fig. 6 shows the response of the system when the initial absolute angular position is equal to [3°, 3°, 3°]. The time (T) taken for the system to stabilize is 6.35 s. The maximum voltage for motor 1 (u_1) and motor 2 (u_2) is 12 V.

7.3 Simulation results of LQR on Robogymnast with disturbance

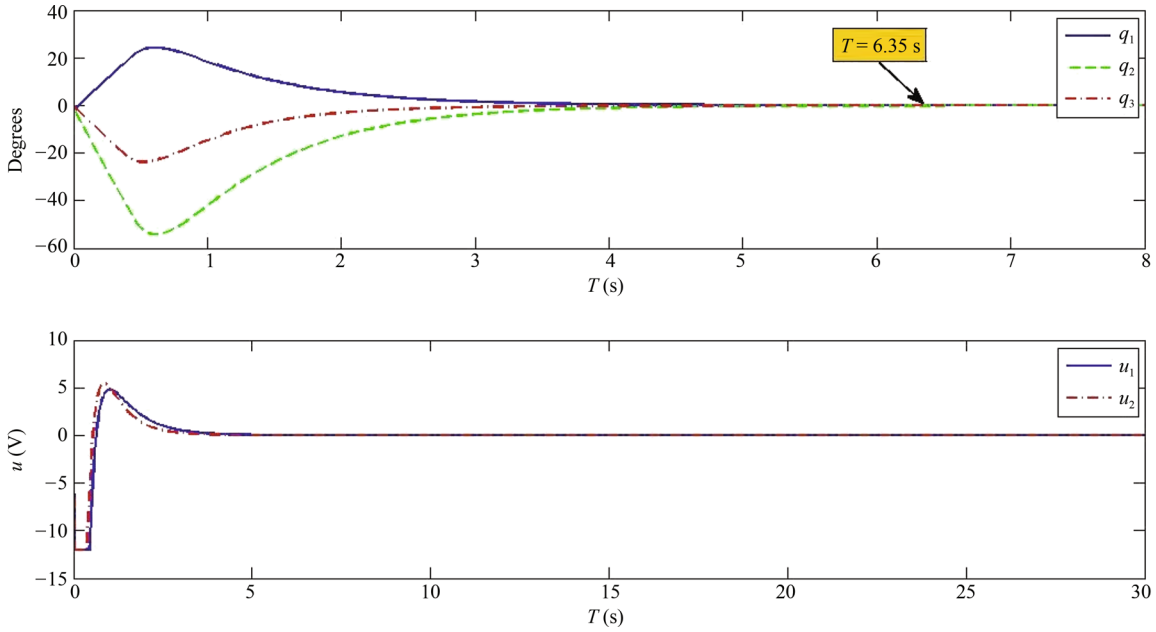

Fig. 4 Simulation of LQR with initial deflection of $\theta_1 = -3°$, $\theta_2 = -3°$, $\theta_3 = -3°$

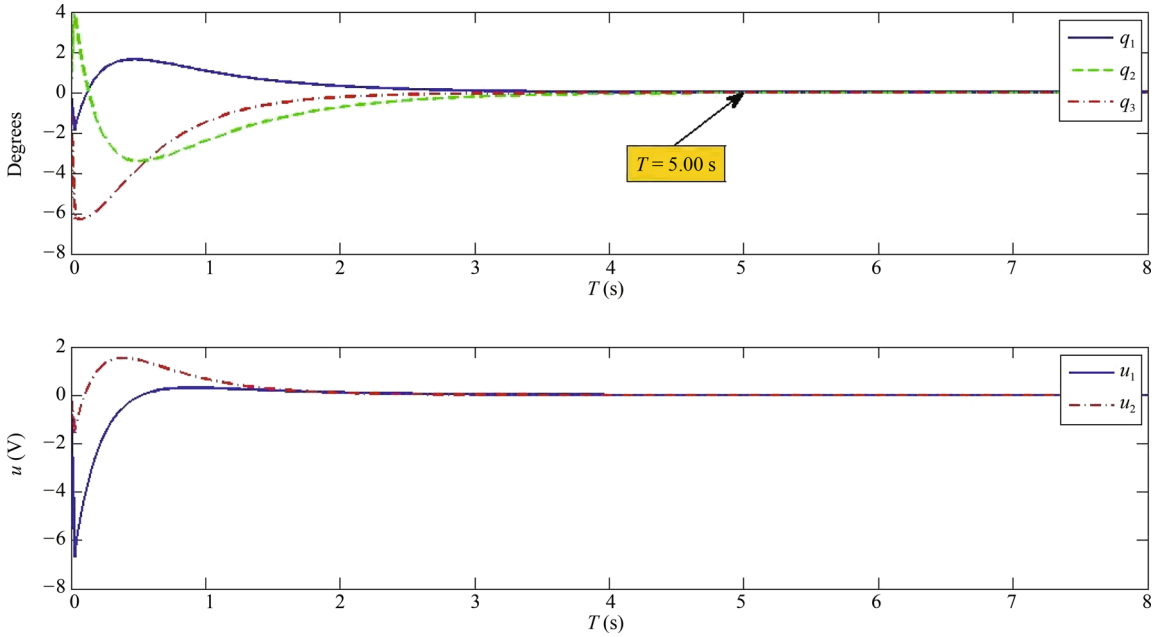

Fig. 5 Simulation of LQR with initial deflection of $\theta_1 = -3°$, $\theta_2 = 3°$, $\theta_3 = -3°$

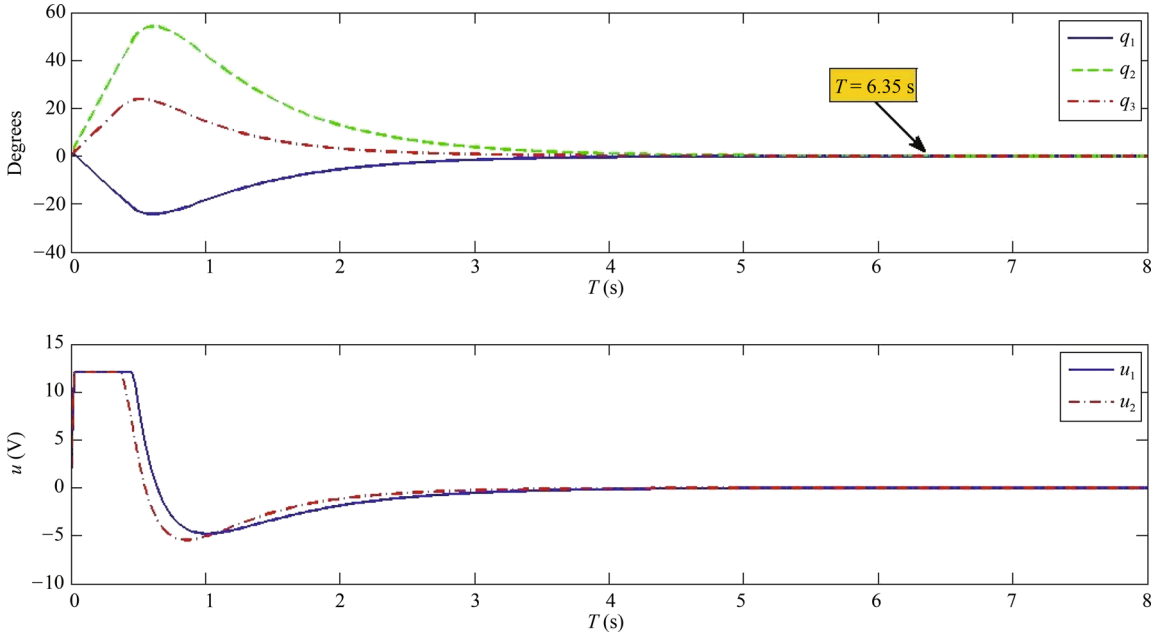

Fig. 6 Simulation of LQR with initial deflection of $\theta_1 = 3°$, $\theta_2 = 3°$, $\theta_3 = 3°$

A simulated external disturbance was applied to each of the Robogymnast links one at a time and its reaction is observed. The disturbance is applied approximately 2 s after the controller attempts to stabilize the system from an initial absolute angular position equal to [1.5°, 1.5°, 1.5°]. The objective of this test is to determine the robustness of the LQR controller with the parameters obtained using WCMIWO.

Fig. 7 illustrates that when a disturbance is applied to the first link the controller reacts to counter the displacement quickly. The figure reveals that the amount of work done by both motors is more or less the same. From Fig. 8 it can be seen that the system experiences a significant displacement when a disturbance is applied to the second link. However, despite this the controller is still able to balance the Robogymnast successfully.

Fig. 9 represents the reaction of the system when a disturbance is applied to the third link. The displacement in this figure is far less severe when compared to Figs. 7 and 8. It can also be seen that when the disturbance is applied u_1 is significantly larger than u_2. This indicates that most of the work is done by motor 1.

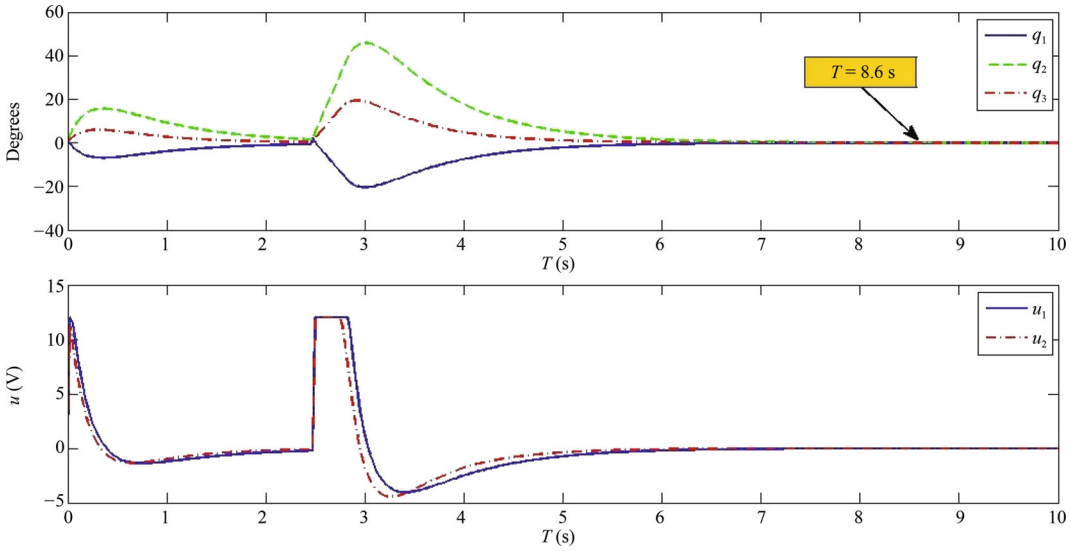

Fig. 7 Disturbance to Link 1

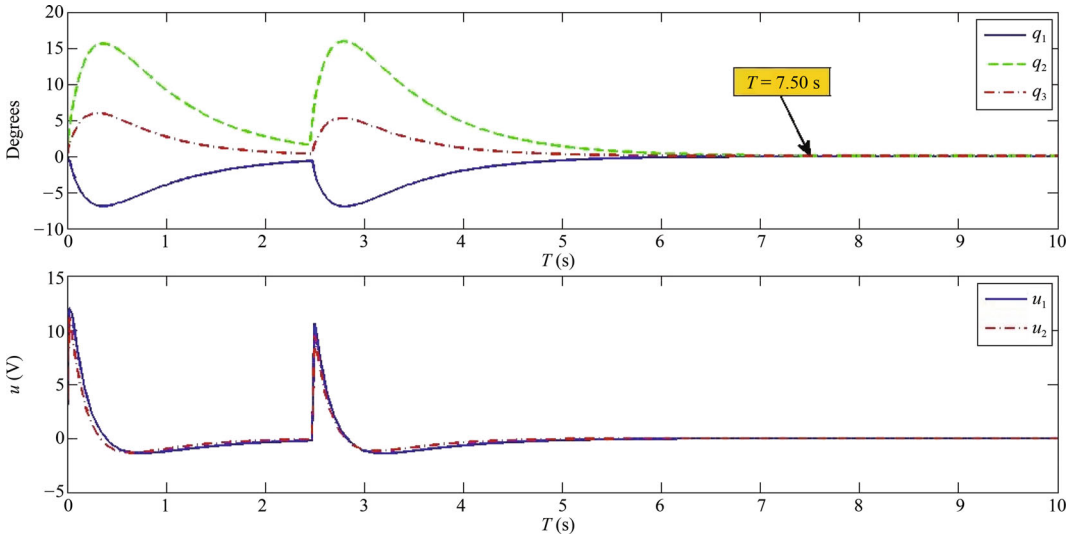

Fig. 8 Disturbance to Link 2

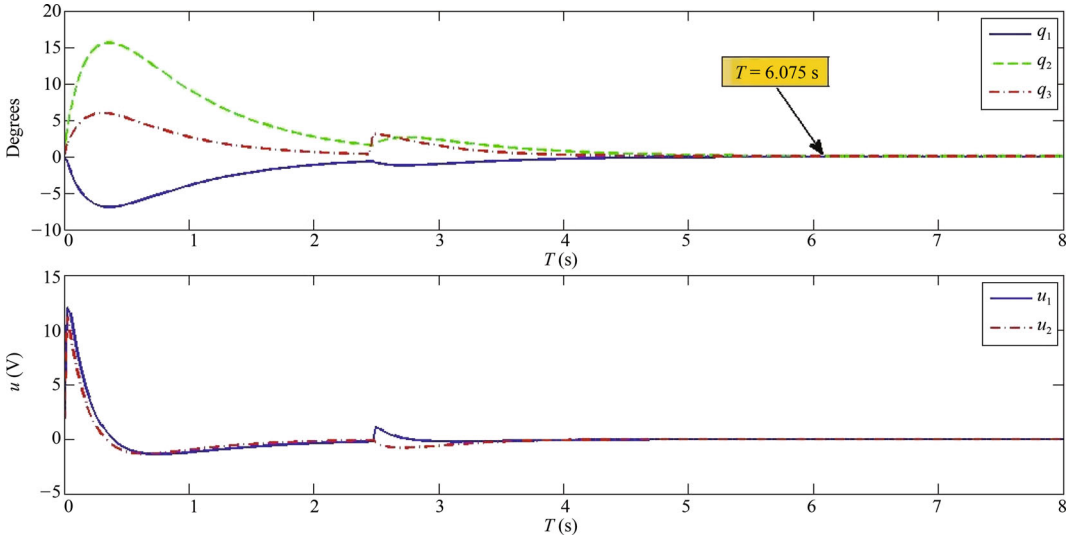

Fig. 9 Disturbance to Link 3

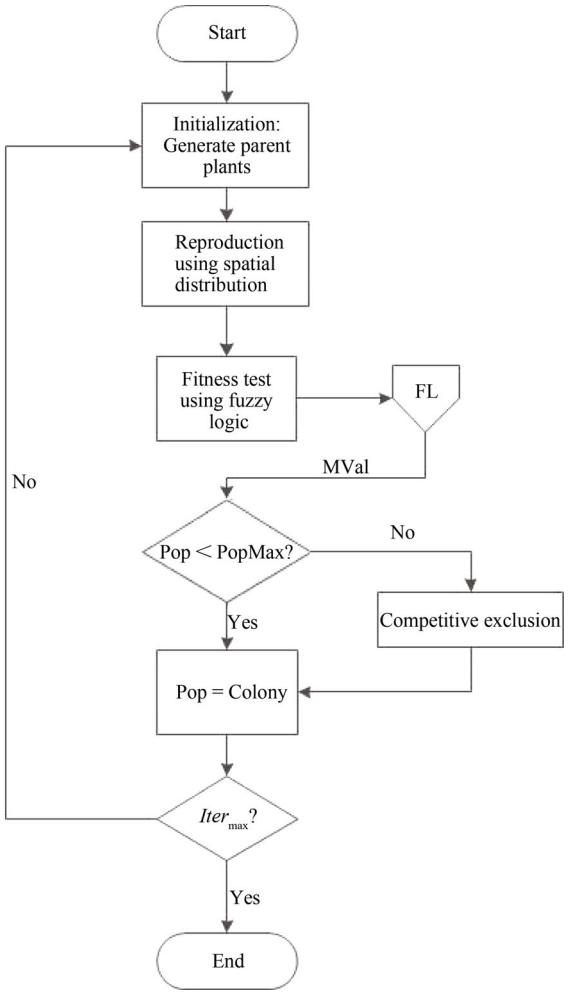

Fig. 10 Main flowchart of the FLIWOH algorithm

8 Fuzzy logic invasive weed optimization hybrid

In this section, a multi-objective fuzzy logic invasive weed optimization hybrid (FLIWOH) technique is proposed. This technique uses a combination of the IWO and fuzzy logic. IWO is used for search and new seeds generation. Fuzzy logic is used to determine the fitness of the seeds by evaluating the fitness memberships of the JT criteria. The flowchart of FLIWOH algorithm and fuzzy logic algorithm are illustrated in Figs. 10 and 11, respectively. The fuzzy logic processor consists of two input variables and one output variable. Each of the input variables, J and T, has three membership functions (Low, AVG High) defined in the range of $[0, 1]$ through normalization (Fig. 12). The boundaries of the three memberships have to be calculated at each iteration using (12)−(21) due to the changing range of the seed variables at each iteration. The output variable consists of three membership functions (NG, AVG, G) within the range of $[0, 5]$.

Two well-known fuzzy rule-based inference systems are Mamdani fuzzy method and the Takagi-Sugeno (T-S) fuzzy method[24]. The Mamdani method is selected as the fuzzy inference engine due to its expressive power, making it easy to formalize and interpret. Another advantage is that it can be used for both multiple-input-single-output (MISO) and multiple-input-multiple-output (MIMO) systems whereas T-S method can only be used in MISO systems[25]. This allows the Mamdani method to be used in future works when MIMO systems are required. The fuzzy rules in Fig. 12 are then applied and the output membership function generates the output membership value of quality (MVal). The set seeds are then arranged in ascending order based on their MVal values, where the smaller the value of MVal the fitter the set of seeds. The set seeds then go through the rest of the conventional IWO process. Table 3 display the FLIWOH parameters used for this process.

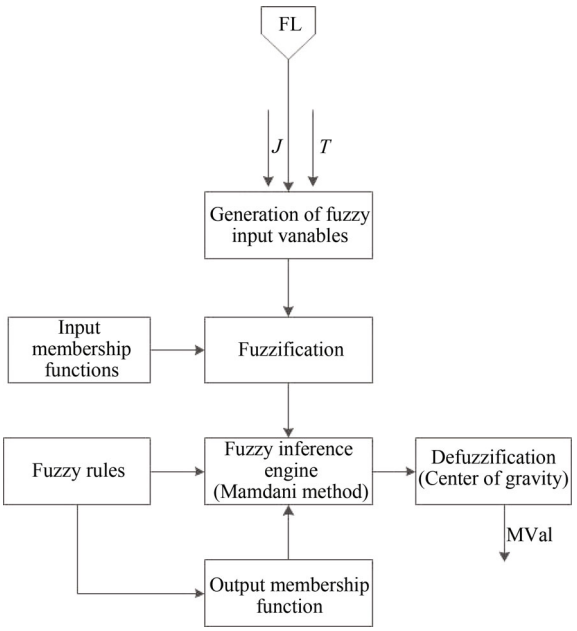

Fig. 11 Flowchart of the fuzzy logic algorithm

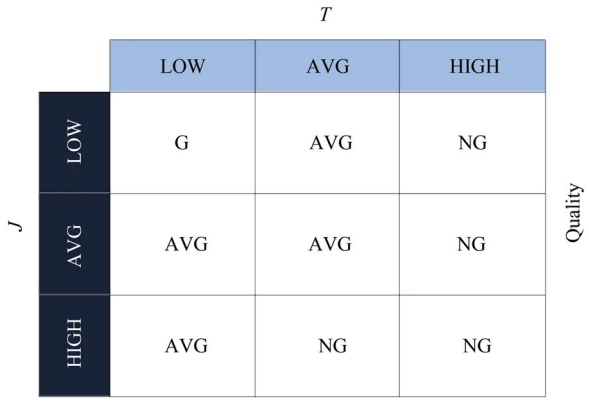

Fig. 12 Fuzzy logic rule

where

$$MedJ = median(J_{norm}) \tag{12}$$

$$UAvgJ = MedJ + (0.25)(MedJ) \tag{13}$$

$$LAvgJ = MedJ - (0.25)(MedJ) \tag{14}$$

Table 3 FLIWOH parameters

Variable	Value	Description
Number of initial plants	5	Number of randomly chosen values from the solution space
Minimum number of seeds	1	Minimum population of solutions
Maximum number of seeds	500	Maximum population of solutions
Initial value of standard deviation	50	Standard deviation used for spatial distribution of plants
Final value of standard deviation	0.5	Final standard deviation used for spatial distribution of plants
Maximum number of iterations	10	Number of iterations
Nonlinear Modulation Index	0.01	–
Target angle	$q_1 \leq 0.001$ rad $q_2 \leq 0.001$ rad $q_3 \leq 0.001$ rad	The angle where time is recorded and used as the fitness criterion
Search range	0 – 1000	Search range used based on trial and error

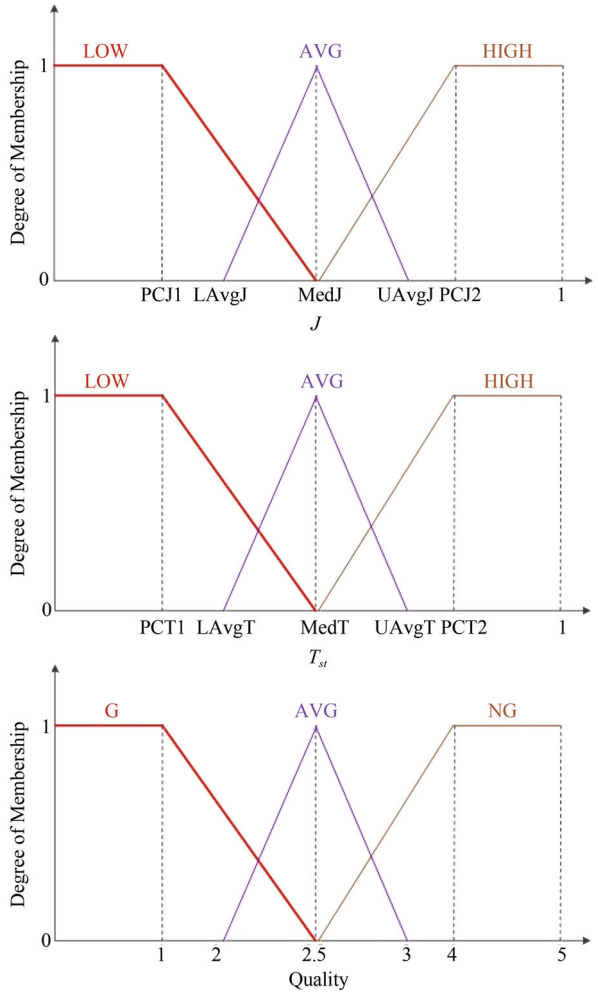

Fig. 13 Fuzzy logic membership functions

$$PCJ1 = (0.25)(MedJ) \tag{15}$$

$$PCJ2 = 1 - PCJ1 \tag{16}$$

$$MedT = medianT_{norm} \tag{17}$$

$$UAvgT = MedT + (0.25)(MedT) \tag{18}$$

$$LAvgT = MedT - (0.25)(MedT) \tag{19}$$

$$PCT1 = 0.25(MedT) \tag{20}$$

$$PCT2 = 1 - PCT1. \tag{21}$$

Fig. 14 shows the fuzzy rules based on the membership functions shown in Fig. 13:

1) IF J is HIGH and T is HIGH THEN Q is NG
2) IF J is AVG and T is HIGH THEN Q is NG
3) IF J is LOW and T is HIGH THEN Q is NG
4) IF J is HIGH and T is AVG THEN Q is NG
5) IF J is AVG and T is AVG THEN Q is AVG
6) IF J is LOW and T is AVG THEN Q is AVG
7) IF J is HIGH and T is LOW THEN Q is AVG
8) IF J is AVG and T is LOW THEN Q is AVG
9) IF J is LOW and T is LOW THEN Q is G

Fig. 14 Fuzzy rules of the membership functions

8.1 Simulation results

Table 4 shows the fittest seeds obtained using FLIWOH. $S_1 = 50.348$, $S_2 = 500.587$, $S_3 = 400.658$, $S_4 = 250.002$, $S_5 = 150.174$ and $S_6 = 100.002$ are selected for analysis. Using (7), the Q matrix obtained from the seeds is

$$Q = \begin{bmatrix} 0.119 \times 10^3 & 0 & 0 & 0 & 0 & 0 \\ 0 & 10.192 \times 10^3 & 0 & 0 & 0 & 0 \\ 0 & 0 & 6.478 \times 10^3 & 0 & 0 & 0 \\ 0 & 0 & 0 & 2.580 \times 10^3 & 0 & 0 \\ 0 & 0 & 0 & 0 & 0.957 \times 10^3 & 0 \\ 0 & 0 & 0 & 0 & 0 & 0.427 \times 10^3 \end{bmatrix}$$

and the corresponding gain matrix is

$$K = \begin{bmatrix} -508.218 & -217.220 & -26.599 & 92.874 & 48.886 & 6.077 \\ -390.619 & -175.107 & 6.822 & 71.843 & 37.837 & 4.603 \end{bmatrix}.$$

The parameters obtained are subjected to the same tests as the WCMIWO parameters.

Fig. 15 illustrates the controlled system response and the voltages when the Robogymnast is in the upright position with the initial absolute angular position equal to [–3°, –3°, –3°]. The maximum voltage u_1 is 12 V and while u_2 is significantly lower at 5.815 9 V. It can be seen that the time taken to reach a stable upright position is 6.375 s.

Fig. 16 shows the response of the system when the initial absolute angular position is equal to [–3°, 3°, –3°]. The time (T) taken for the system to stabilize is 4.05 s. The maximum voltage u_1 is 6.746 2 V and for u_2 is 0.990 9 V.

Table 4 FLIWOH results

S_1	S_2	S_3	S_4	S_5	S_6	Time to reach the upright position (s)	J×10^5	MVal
10.913	100.958	80.485	50.792	30.934	20.655	6.45	9.303	0.915 2
199.492	179.689	200.470	100.651	70.476	89.536	7.15	48.715	0.915 3
209.155	179.445	220.230	120.411	50.526	69.640	6.78	45.249	0.915 3
198.819	119.370	130.565	60.785	50.326	29.608	6.43	19.457	0.915 5
168.432	199.197	228.200	109.943	60.412	138.827	6.75	57.387	0.915 7
208.685	199.507	258.648	110.460	50.711	120.046	6.20	54.100	0.915 9
120.759	190.756	260.140	130.647	50.894	160.390	7.45	59.624	0.923 0
120.402	190.430	259.515	130.373	50.824	159.905	7.45	59.389	0.923 2
120.694	190.363	259.617	130.451	50.829	159.998	7.45	59.418	0.923 2
169.558	199.771	260.114	150.629	40.731	150.223	7.35	66.869	0.926 3

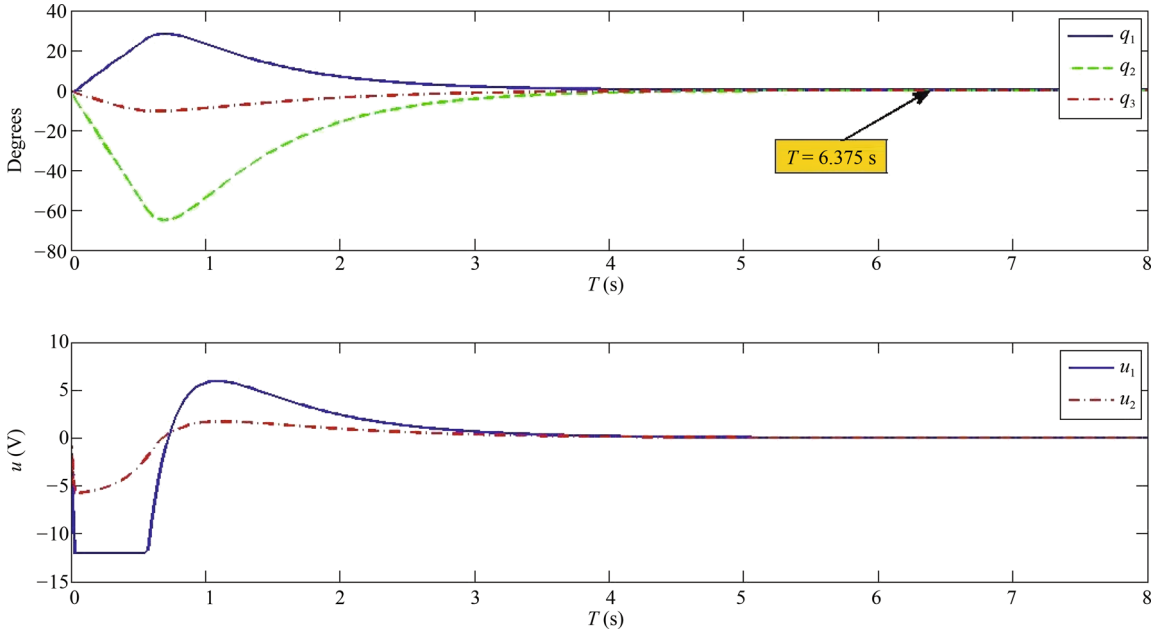

Fig. 15 Simulation of LQR with initial deflection of $\theta_1 = -3°$, $\theta_2 = -3°$, $\theta_3 = -3°$

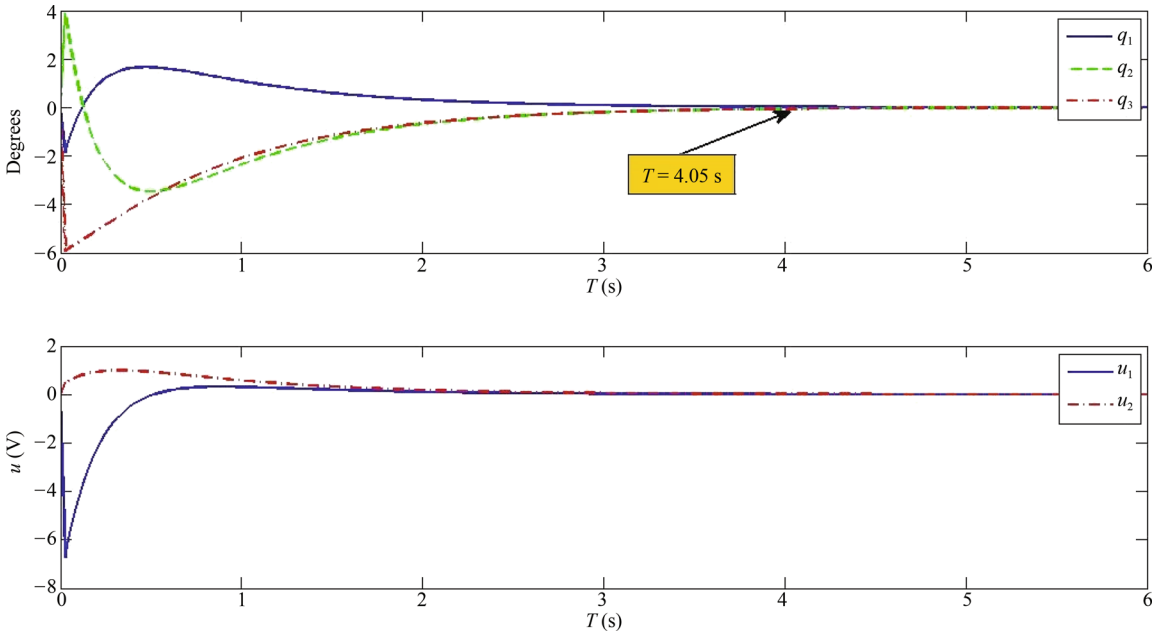

Fig. 16 Simulation of LQR with initial deflection of $\theta_1 = -3°$, $\theta_2 = 3°$, $\theta_3 = -3°$

Fig. 17 illustrates the controller′s ability to stabilize the Robogymnast when it is in the upright position with the initial absolute angular position equal to [3°, 3°, 3°]. The maximum voltage for the motor 1 (u_1) is 12 volts and motor 2 (u_2) 5.815 9 volts. It can be seen that the time taken to reach a stable upright position is 6.37 s.

8.2 Simulation results of LQR on Robogymnast with disturbance

A simulated external disturbance was applied to each of the Robogymnast links one at a time and its reaction is observed. The disturbance is applied 2 s after the controller attempts to stabilize the system from an initial absolute angular position equal to [1.5°, 1.5°, 1.5°].

Fig. 18 shows the effect a disturbance has on the system when applied to the first link. The system was able to counter the disturbance and stabilize itself successfully. Voltage u_1 is more than double of voltage u_2 thus showing that most of the work is done by motor 1.

Fig. 19 depicts the controllers successful attempt to balance the Robogymnast when a disturbance is applied to the second link. It can be seen that motor 1 requires significantly larger voltage compared to motor 2. The controller is able to stabilize the robot in 7.375 s.

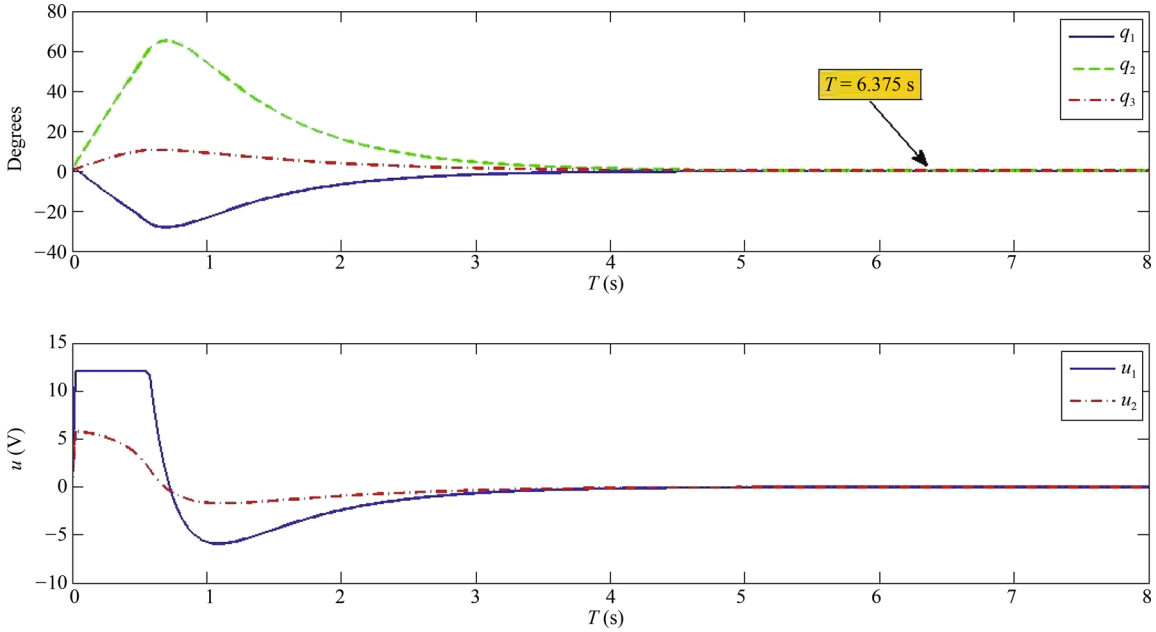

Fig. 17 Simulation of LQR with initial deflection of $\theta_1 = 3°$, $\theta_2 = 3°$, $\theta_3 = 3°$

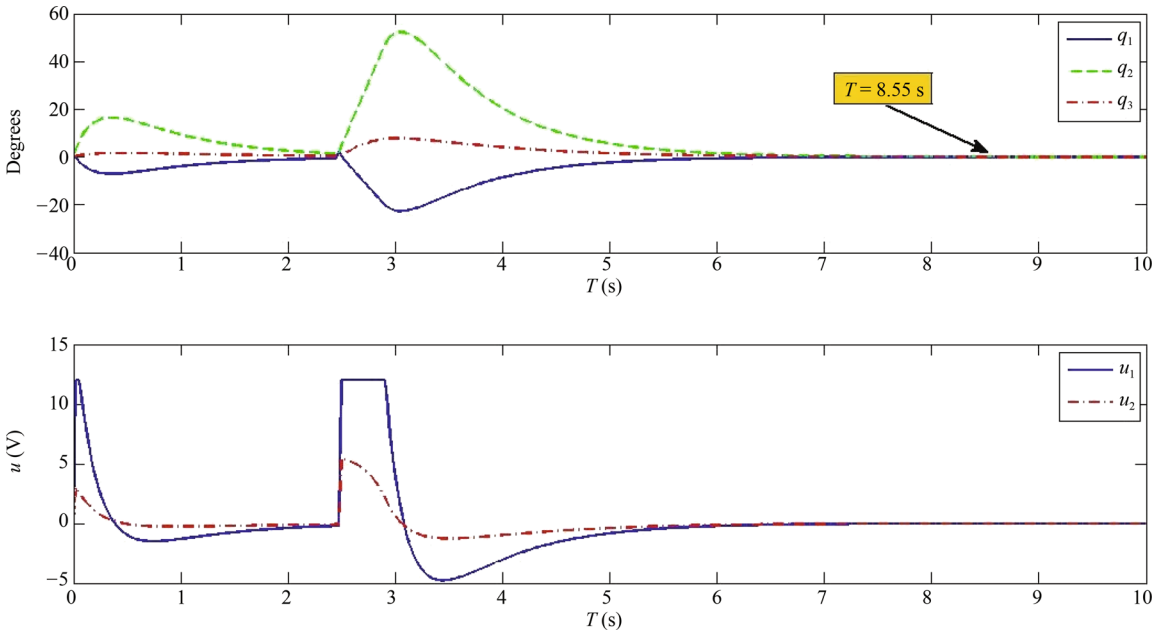

Fig. 18 Disturbance to Link 1

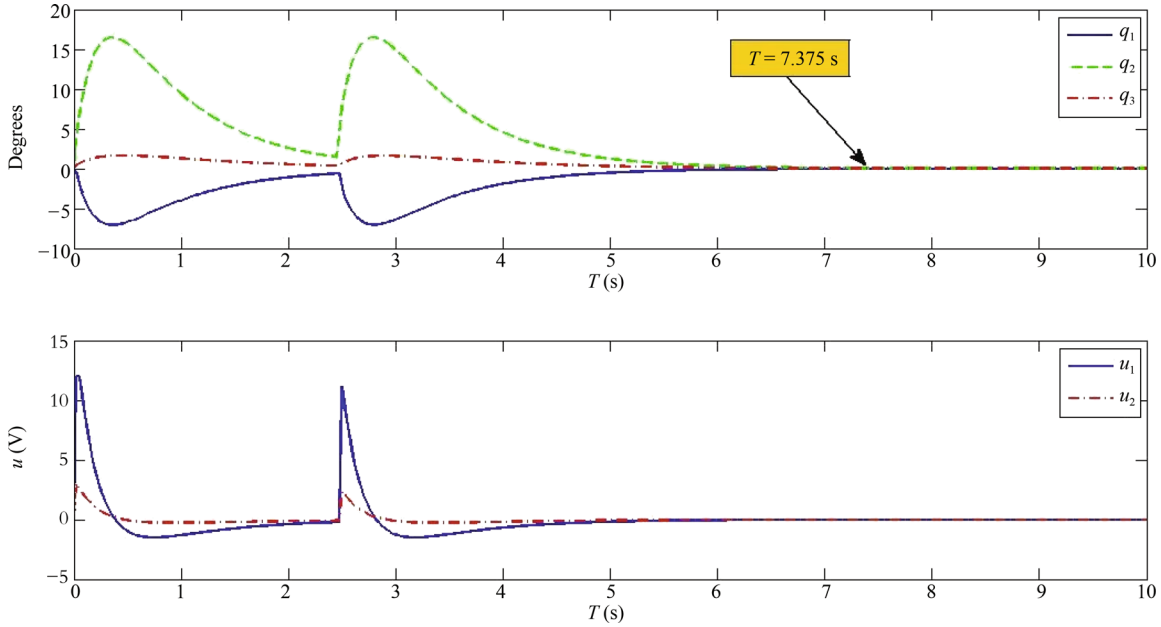

Fig. 19 Disturbance to Link 2

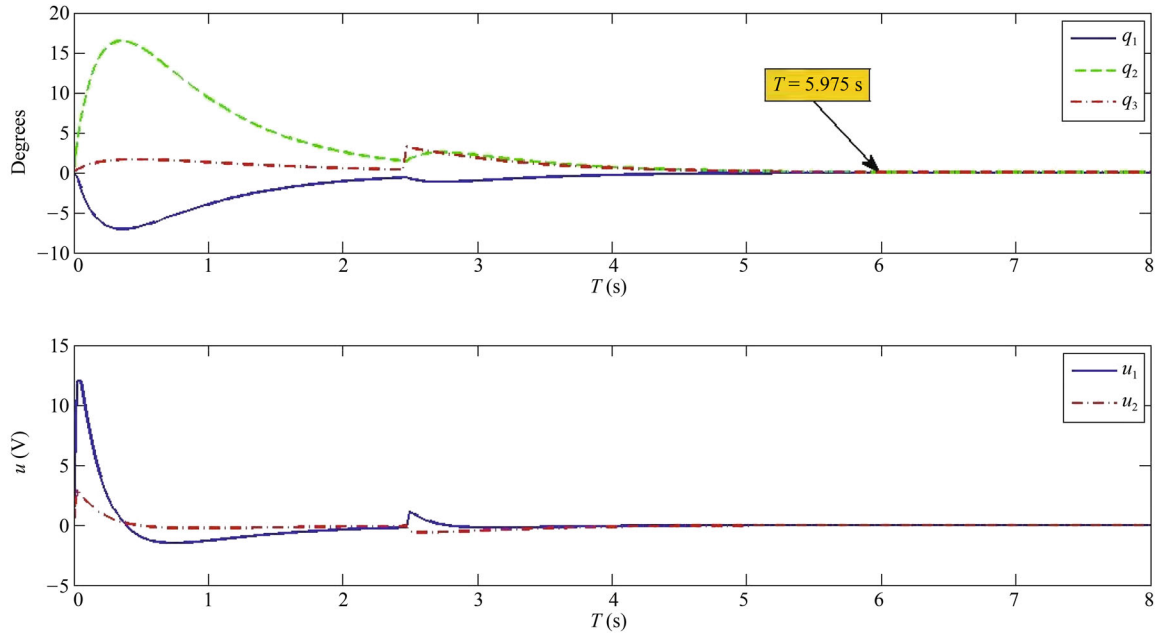

Fig. 20 Disturbance to Link 3

Fig. 20 displays the reaction of the system when a disturbance is applied to the third link. The displacement caused by the system is minor thus requiring very small voltages for both motors.

9 Training with disturbance

In this section the optimization procedures in Sections 7 and 8 are repeated with minor disturbance applied to the system model. The disturbance consists of random values between the range [0.01, 0.05] which were multiplied with previous states and added to the present states. This is to simulate the application of external disturbance on the system. It is expected that the increased difficulty in the optimization process would generate seeds that would perform much better when applied to the system without disturbance.

9.1 WCMIWO training with disturbance results

Seeds $S_1 = 28.398$, $S_2 = 26.475$, $S_3 = 29.353$, $S_4 = 11.210$, $S_5 = 6.811$ and $S_6 = 10.833$ are selected for analysis. Using (7), the matrix Q obtained from the seeds is

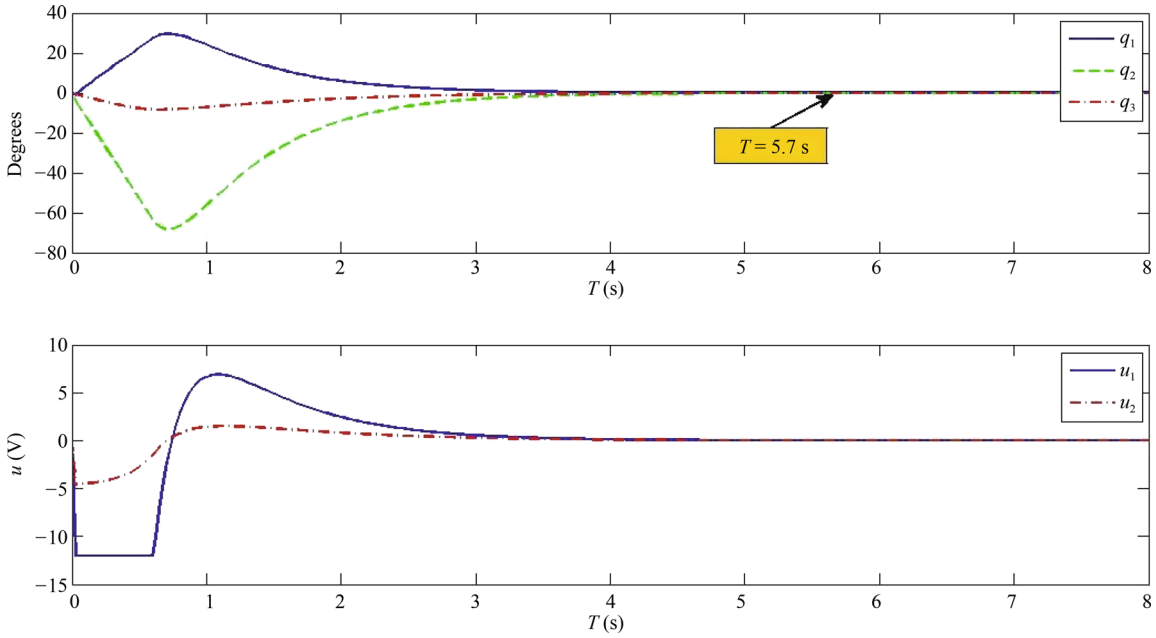

Fig. 21 Simulation of LQR with initial deflection of $\theta_1=-3°$, $\theta_2=-3°$, $\theta_3=-3°$

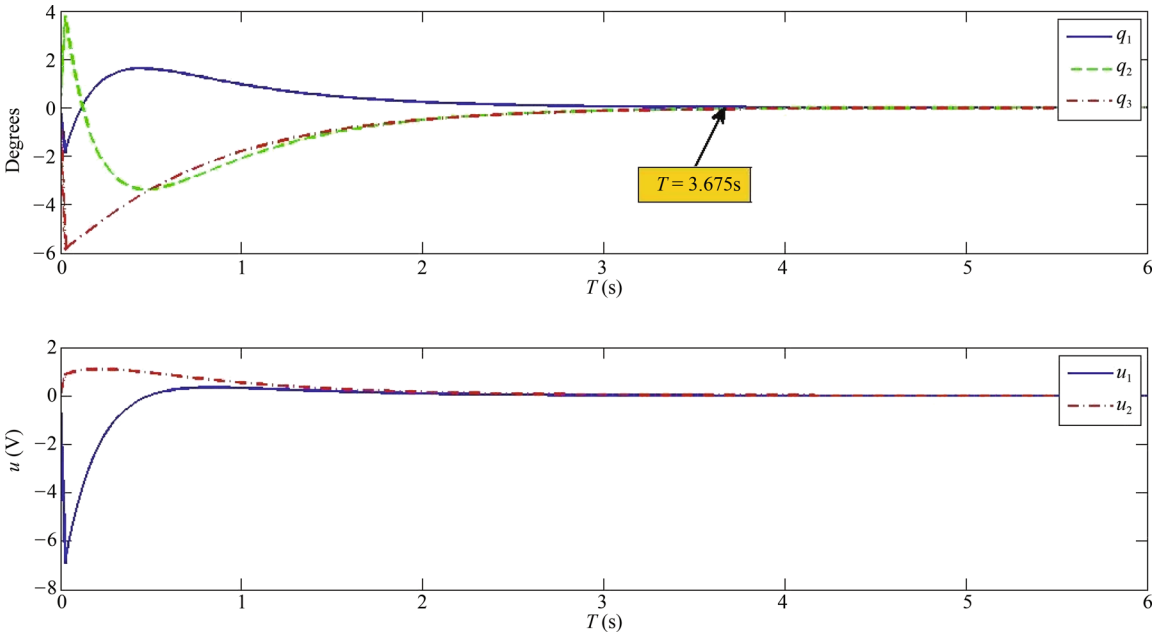

Fig. 22 Simulation of LQR with initial deflection of $\theta_1=-3°$, $\theta_2=3°$, $\theta_3=-3°$

$$Q=\begin{bmatrix} 806.435 & 0 & 0 & 0 & 0 & 0 \\ 0 & 700.912 & 0 & 0 & 0 & 0 \\ 0 & 0 & 861.568 & 0 & 0 & 0 \\ 0 & 0 & 0 & 125.658 & 0 & 0 \\ 0 & 0 & 0 & 0 & 46.392 & 0 \\ 0 & 0 & 0 & 0 & 0 & 117.351 \end{bmatrix}$$

and the corresponding gain matrix is

$$K=\begin{bmatrix} -551.762 & -237.628 & -27.863 & 100.860 & 53.093 & 6.594 \\ -88.009 & -39.687 & 12.589 & 16.188 & 8.531 & 1.005 \end{bmatrix}.$$

Figs. 21–23 represents the behavior of the system when the LQR controller trained using WCMIWO with disturbance is applied.

9.2 FLIWOH with disturbance results

Fittest seeds $S_1 = 25.065\,9$, $S_2 = 16.982\,1$, $S_3 = 24.798\,8$, $S_4 = 8.711\,9$, $S_5 = 3.821\,2$ and $S_6 = 9.928\,0$ are selected for analysis. Using (7), the matrix Q obtained from the seeds is

$$Q=\begin{bmatrix} 628.298 & 0 & 0 & 0 & 0 & 0 \\ 0 & 288.392 & 0 & 0 & 0 & 0 \\ 0 & 0 & 614.982 & 0 & 0 & 0 \\ 0 & 0 & 0 & 75.898 & 0 & 0 \\ 0 & 0 & 0 & 0 & 14.602 & 0 \\ 0 & 0 & 0 & 0 & 0 & 98.566 \end{bmatrix}$$

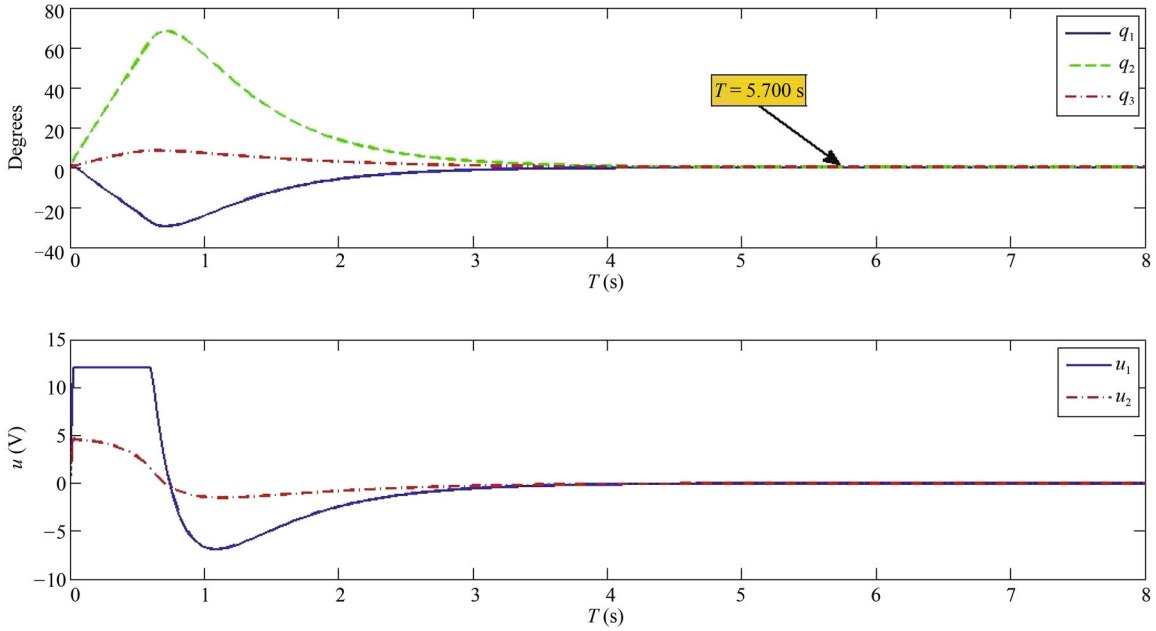

Fig. 23 Simulation of LQR with initial deflection of $\theta_1 = -3°$, $\theta_2 = 3°$, $\theta_3 = 3°$

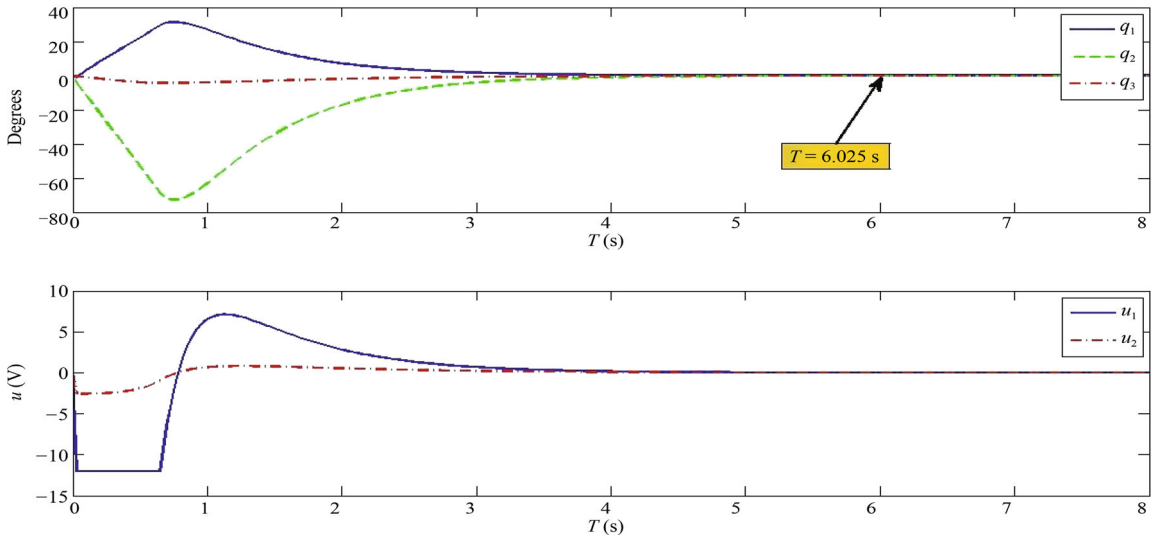

Fig. 24 Simulation of LQR with initial deflection of $\theta_1 = -3°$, $\theta_2 = -3°$, $\theta_3 = -3°$

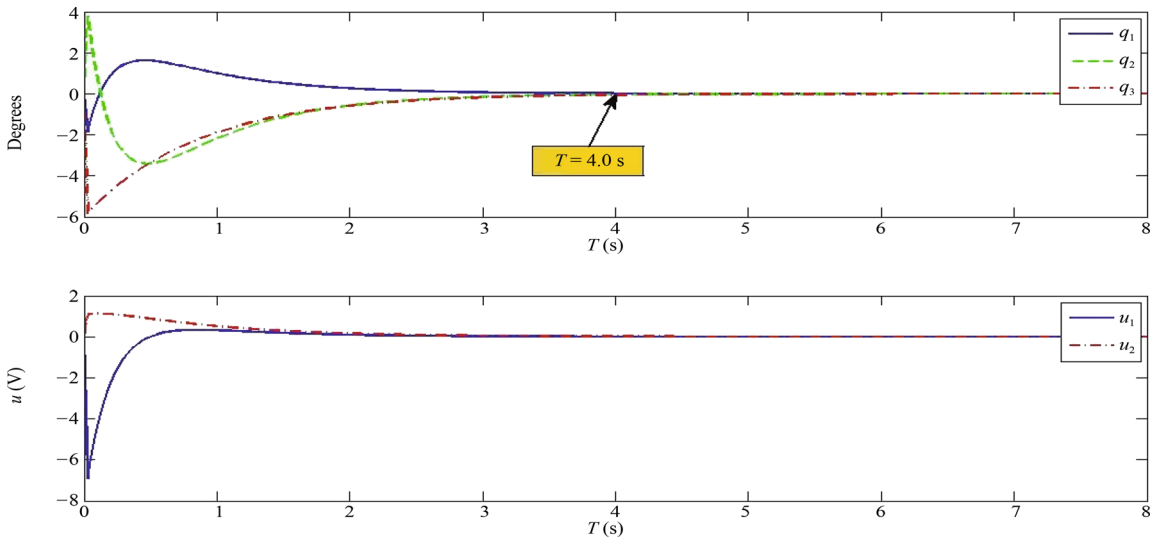

Fig. 25 Simulation of LQR with initial deflection of $\theta_1 = -3°$, $\theta_2 = 3°$, $\theta_3 = -3°$

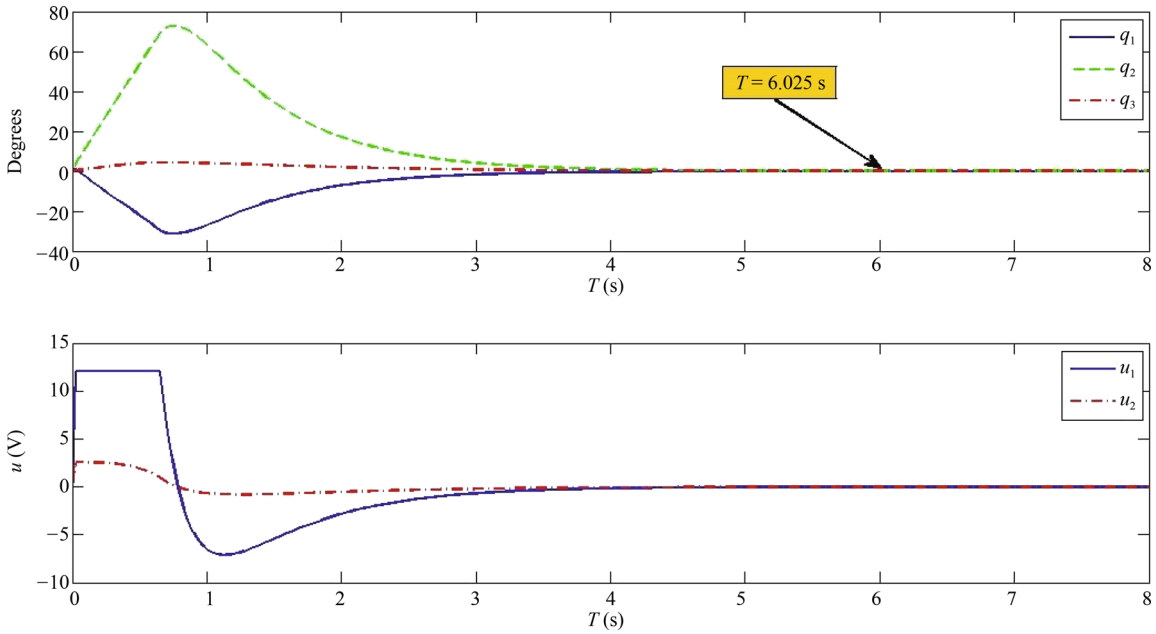

Fig. 26 Simulation of LQR with initial deflection of $\theta_1 = -3°$, $\theta_2 = 3°$, $\theta_3 = 3°$

and the corresponding gain matrix is

$$K=\begin{bmatrix} -550.753 & -236.967 & -27.567 & 100.860 & 52.969 & 6.578 \\ -49.551 & -22.202 & 12.866 & 9.132 & 4.814 & 0.550 \end{bmatrix}$$

Figs. 20–26 represents the behavior of the system when the LQR controller trained using FLIWOH with disturbance is applied.

10 Discussion

The simulation results proved that the designed LQR controller using parameters obtained by both methods can successfully bring the Robogymnast to an inverted and stable configuration. WCMIWO and FLIWOH produced LQR controllers that have similar reaction times to each other but are slower compared to the LQR controllers trained with disturbance. The WCMIWO LQR controller uses slightly less voltage for motor 1 (u_1) compared to the other methods. However, it requires higher voltage for motor 2 (u_2) when compared to the other methods with FLIWOH with disturbance requiring the least amount of voltage (u_2) for motor 2 in almost all configurations. This result is consistent throughout the three configurations. In order to further analyze the performance of the controllers, more tests had to be done. Tables 5 – 14 show the performance comparison of both controllers in different initial angular configurations.

Tables 5–14 show that all the controllers trained with disturbance achieved faster settling time compared to their counter-parts that were not trained with disturbance. At small angles voltage u_1 is lower for WCMIWO but at large angles the difference cease to exist. Voltage u_2 is lower for FLIWOH trained with disturbance in almost all configurations. Both controllers that were trained with disturbance were unable to recover the Robogymnast when the initial

Table 5 Comparison of performance for deflection angle of $\theta_1 = 1°$, $\theta_2 = 1°$, $\theta_3 = 1°$

Method	J_{sum}	$T_{\max}$ (s)	$u_{1\max}$ (V)	$u_{2\max}$ (V)
WCMIWO	1 313 100	4.775	8.866	7.457
FLIWOH	1 649	4.600	9.272	1.939
WCMIWO with disturbance	3 449	4.075	9.630	1.536
FLIWOH with disturbance	1 745	4.250	9.613	0.865

Table 6 Comparison of performance for deflection angle of $\theta_1 = 1°$, $\theta_2 = -1°$, $\theta_3 = 1°$

Method	J_{sum}	$T_{\max}$ (s)	$u_{1\max}$ (V)	$u_{2\max}$ (V)
WCMIWO	72 391	3.175	2.221	0.517
FLIWOH	94	3.125	2.249	0.330
WCMIWO with disturbance	196	2.850	2.308	0.366
FLIWOH with disturbance	109	3.050	2.30	30.374

Table 7 Comparison of performance for deflection angle of $\theta_1 = 3°$, $\theta_2 = 3°$, $\theta_3 = 3°$

Method	J_{sum}	$T_{\max}$ (s)	$u_{1\max}$ (V)	$u_{2\max}$ (V)
WCMIWO	22 296 000	6.35	12.000	12.000
FLIWOH	34 779	6.375	12.000	5.816
WCMIWO with disturbance	81 669	5.700	12.000	4.608
FLIWOH with disturbance	44 946	6.025	12.000	2.595

absolute angular position is equal to [5.45°, 0°, 0°]. Further test shows that WCMIWO trained with disturbance can recover from a maximum initial angular position of [5.432°, 0°, 0°] while FLIWOH trained with disturbance can only recover from the initial angular position of [5.369°, 0°, 0°]. WCMIWO and FLIWOH can recover from a maximum initial angular position of [5.692°, 0°, 0°].

Table 8 Comparison of performance for deflection angle of $\theta_1 = 3°$, $\theta_2 = -3°$, $\theta_3 = 3°$

Method	J_{sum}	T_{max} (s)	$u_{1\,max}$ (V)	$u_{2\,max}$ (V)
WCMIWO	651 520	4.075	6.662	1.550
FLIWOH	843	4.050	6.746	0.991
WCMIWO with disturbance	1 766	3.675	6.924	1.097
FLIWOH with disturbance	979	4.000	6.909	1.121

Table 9 Comparison of performance for deflection angle of $\theta_1 = 3.1°$, $\theta_2 = 3.1°$, $\theta_3 = 3.1°$

Method	J_{sum}	T_{max} (s)	$u_{1\,max}$ (V)	$u_{2\,max}$ (V)
WCMIWO	28 180 000	6.525	12.000	12.000
FLIWOH	49 311	6.650	12.000	6.010
WCMIWO with disturbance	123 270	6.025	12.000	4.762
FLIWOH with disturbance	77 390	6.475	12.000	2.700

Table 10 Comparison of performance for deflection angle of $\theta_1 = 0°$, $\theta_2 = 4°$, $\theta_3 = 5°$

Method	J_{sum}	T_{max} (s)	$u_{1\,max}$ (V)	$u_{2\,max}$ (V)
WCMIWO	4 526 100	5.375	12.000	12.000
FLIWOH	5 752	5.200	12.000	3.298
WCMIWO with disturbance	12 349	4.600	12.000	2.551
FLIWOH with disturbance	6 220	4.800	12.000	1.325

Table 11 Comparison of performance for deflection angle of $\theta_1 = 4°$, $\theta_2 = 0°$, $\theta_3 = 0°$

Method	J_{sum}	T_{max} (s)	$u_{1\,max}$ (V)	$u_{2\,max}$ (V)
WCMIWO	7 485 100	5.575	12.000	12.000
FLIWOH	9 819	5.450	12.000	4.277
WCMIWO with disturbance	20 920	4.825	12.000	3.374
FLIWOH with disturbance	10 680	5.050	12.000	1.909

Table 12 Comparison of performance for deflection angle of $\theta_1 = 5.45°$, $\theta_2 = 0°$, $\theta_3 = 0°$

Method	J_{sum}	T_{max} (s)	$u_{1\,max}$ (V)	$u_{2\,max}$ (V)
WCMIWO	33 873 000	6.700	12.000	12.000
FLIWOH	1 411 751	6.800	12.000	12.000
WCMIWO with disturbance	Inf	Inf	12.000	12.000
FLIWOH with disturbance	Inf	Inf	12.000	12.000

Table 13 Comparison of performance for deflection angle of $\theta_1 = 5.65°$, $\theta_2 = 0°$, $\theta_3 = 0°$

Method	J_{sum}	T_{max} (s)	$u_{1\,max}$ (V)	$u_{2\,max}$ (V)
WCMIWO	71 745 000	7.375	12.000	12.000
FLIWOH	2 978 200	7.500	12.000	12.000
WCMIWO with disturbance	Inf	Inf	12.000	12.000
FLIWOH with disturbance	Inf	Inf	12.000	12.000

Table 14 Comparison of performance for deflection angle of $\theta_1 = 5.7°$, $\theta_2 = 0°$, $\theta_3 = 0°$

Method	J_{sum}	T_{max} (s)	$u_{1\,max}$ (V)	$u_{2\,max}$ (V)
WCMIWO	Inf	Inf	12.000	12.000
FLIWOH	Inf	Inf	12.000	12.000
WCMIWO with disturbance	Inf	Inf	12.000	12.000
FLIWOH with disturbance	Inf	Inf	12.000	12.000

Based on Table 15, WCMIWO LQR controller has the highest ranking for efficiency of motor 1 and ability to upright from larger initial angles. This makes it the most suitable controller for this application largely due to the fact that the systems dependency on u_1 to maintain the Robogymnast in an upright position is larger than u_2. This can be seen from the results where u_1 is usually larger than u_2. Since both u_1 and u_2 have a maximum limit of 12 V, it is of high interest that the required value of u_1 be as small as possible.

Table 15 Ranking of performance

Method	Settling time	Efficiency (u_1) of motor 1	Efficiency (u_2) of motor 2	Ability to be upright from larger initial angles of deflection
WCMIWO	4	1	4	1
FLIWOH	3	2	3	1
WCMIWO with disturbance	1	3	2	2
FLIWOH with disturbance	2	3	1	3

For further evaluation, the performances of the controllers are compared with two state of the art controllers, the discrete LQR (DLQR) and LQR with local control (LQR+LC). The DLQR and LQR+LC are two controllers designed by Kamil[26]. The two controllers are suitable candidates for comparison with the proposed four controllers due to the fact that their performance was evaluated using the same test bench (Robogymnast). The comparison is done based on results obtained from [26]. Tables 16–18 show the comparison results.

Table 16 Comparison of performance for deflection angle of $\theta_1 = 1.1°$, $\theta_2 = 0.9°$, $\theta_3 = 0.8°$

Method	$T_{\max}$ (s)	$u_{1\max}$ (V)	$u_{2\max}$ (V)
WCMIWO	4.750	8.948	7.546
FLIWOH	4.850	8.925	6.9
WCMIWO with disturbance	4.075	9.715	1.573
FLIWOH with disturbance	4.250	9.698	0.896
DLQR	10.000	10.000	3.00
LQR + LC	1.500	10.000	0.025

Table 17 Comparison of performance for deflection angle of $\theta_1 = 1.3°$, $\theta_2 = 1.5°$, $\theta_3 = -5°$

Method	$T_{\max}$ (s)	$u_{1\max}$ (V)	$u_{2\max}$ (V)
WCMIWO	4.775	9.246	10.000
FLIWOH	4.875	9.272	10.000
WCMIWO with disturbance	4.050	10.000	3.564
FLIWOH with disturbance	4.225	10.000	2.661
DLQR	10.000	10.000	5.200
LQR + LC	10.000	10.000	1.400

Table 18 Comparison of performance for deflection angle of $\theta_1 = 1°$, $\theta_2 = 1.1°$, $\theta_3 = 1.2°$

Method	$T_{\max}$ (s)	$u_{1\max}$ (V)	$u_{2\max}$ (V)
WCMIWO	4.800	9.292	7.780
FLIWOH	4.875	9.296	7.111
WCMIWO with disturbance	4.100	10.000	1.583
FLIWOH with disturbance	4.300	10.000	0.881
DLQR	9.000	10.000	2.700
LQR + LC	1.500	10.000	0.038

LQR + LC has the overall fastest settling time while DLQR has the slowest settling time. WCMIWO is the most efficient in terms of power for motor 1 while LQR with LC is the most efficient for motor 2.

At the early stage of the WCMIWO and FLIWOH process, exploration is prioritized to obtain an estimate of the region of where the optimal solution is located. As the number of iterations increases, exploitation begins to take precedent as the estimation of the optimal solutions location improves.

11 Conclusions

The purpose of this paper was to determine if the multi-objective IWO could produce a LQR controller that takes into consideration the values of cost function J and settling time (T). The first optimization method applies IWO for WCM optimization of the J and T values. Weights were assigned to each variable and the resulting values were multiplied to each other to produce a single value which is used as the fitness criteria. The second optimization method is a hybrid IWO that employs fuzzy logic to attain a membership value which is used as the fitness criteria. Using the Q values obtained, two LQR controllers were designed and tested using simulation. Two other controllers were designed using the previous two methods but trained with minor disturbances. All four controllers successfully balanced the Robogymnast in an inverted configuration even when external disturbances were applied to it. The four controllers were examined and their performance evaluated against two state of the art controllers (DLQR and LQR with LC).

Acknowledgements

Hafizul Azizi Ismail would like to express the deepest gratitude to Majlis Amanah Rakyat (MARA) and German Malaysian Institute (GMI) for their sponsorship. Finally, Hafizul Azizi Ismail would like to thank my family and friends for their support.

References

[1] S. Takashiro, N. Yoshihiko. Analysis and control of underactuated mechanisms via the averaging method. In *Proceedings of the 2nd Asian Control Conference*, Springer, Seoul, Korea, vol. 1, pp. 273–276, 1997.

[2] L. B. Prasad, B. Tyagi, H. O. Gupta. Optimal control of nonlinear inverted pendulum system using PID controller and LQR: Performance analysis without and with disturbance input. *International Journal of Automation and Computing*, vol. 11, no. 6, pp. 661–670, 2014.

[3] K. J. AAström, K. Furuta. Swinging up a pendulum by energy control. *Automatica*, vol. 36, no. 2, pp. 287–295, 2000.

[4] G. A. Medrano-Cerda, E. E. Eldukhri, M. Cetin. Balancing and attitude control of double and triple inverted pendulums. *Transactions of the Institute of Measurement and Control*, vol. 17, no. 3, pp. 143–154, 1995.

[5] K. Furut, T. Ochiai, N. Ono. Attitude control of a triple inverted pendulum. *International Journal of Control*, vol. 39, no. 6, pp. 1351–1365, 1984.

[6] S. C. Brown, K. M. Passino. Intelligent control for an acrobot. *Journal of Intelligent and Robotic Systems*, vol. 18, no. 3, pp. 209–248, 1997.

[7] H. G. Kamil, E. E. Eldukhri, M. S. Packianather. Balancing control of robot gymnast based on discrete-time linear quadratic regulator technique. In *Proceedings of the 2nd International Conference on Artificial Intelligence, Modelling and Simulation*, IEEE, Madrid, Spain, pp. 137–142, 2014.

[8] K. Deb. Multi-objective optimization. *Search Methodologies*, E. K. Burke, G. Kendall, Eds., New York, USA: Springer, pp. 403–449, 2014.

[9] Y. Li, J. C. Liu, Y. Wang. Design approach of weighting matrices for LQR based on multi-objective evolution algorithm. In *Proceedings of International Conference on Information and Automation*, IEEE, Changsha, China, pp. 1188–1192, 2008.

[10] S. A. Ghoreishi, M. A. Nekoui, S. O. Basiri. Optimal design of LQR weighting matrices based on intelligent optimization methods. *International Journal of Intelligent Information Processing*, vol. 2, no. 1, pp. 63–74, 2008.

[11] S. Das, I. Pan, S. Das. Multi-objective LQR with optimum weight selection to design FOPID controllers for delayed fractional order processes. *ISA Transactions*, vol. 58, pp. 35–49, 2015.

[12] P. Khalaf, H. Richter, A. J. van den Bogert, D. Simon. Multi-objective optimization of impedance parameters in a prosthesis test robot. In *Proceedings of ASME Dynamic Systems and Control Conference*, ASME, Columbus, USA, 2015.

[13] H. Q. Wang, L. Liao, D. Y. Wang, S. J. Wen, M. C. Deng. Improved artificial bee colony algorithm and its application in LQR controller optimization. *Mathematical Problems in Engineering*, vol. 2014, Article No. 695637, 2014.

[14] H. A. Ismail, M. S. Packianather, R. I. Grosvenor, E. E. Eldhukri. The application of IWO in LQR controller design for the Robogymnast. In *Proceedings of SAI Intelligent Systems Conference*, IEEE, London, UK, pp. 274–279, 2015.

[15] E. E. Eldukhri, D. T. Pham. Autonomous swing-up control of a three-link robot gymnast. *Proceedings of the Institution of Mechanical Engineers, Part I: Journal of Systems and Control Engineering*, vol. 224, no. 7, pp. 825–833, 2010.

[16] S. Sehgal, S. Tiwari. LQR control for stabilizing triple link inverted pendulum system. In *Proceedings of the 2nd International Conference on Power, Control and Embedded Systems*, IEEE, Allahabad, India, pp. 1–5, 2012.

[17] E. Lee, J. Perkins. Comparison of techniques for stabilization of a triple inverted pendulum. 2008.

[18] R. T. Marler, J. S. Arora. Survey of multi-objective optimization methods for engineering. *Structural and Multidisciplinary Optimization*, vol. 26, no. 6, pp. 369–395, 2004.

[19] G. P. Rangaiah, A. Bonilla-Petriciolet. *Multi-objective Optimization in Chemical Engineering: Developments and Applications*, New York, USA: John Wiley and Sons, 2013.

[20] K. E. Parsopoulos, M. N. Vrahatis. Particle swarm optimization method in multiobjective problems. In *Proceedings of ACM Symposium on Applied Computing*, ACM, Madrid, Spain, pp. 603–607, 2002.

[21] A. R. Mehrabian, C. Lucas. A novel numerical optimization algorithm inspired from weed colonization. *Ecological Informatics*, vol. 1, no. 4, pp. 355–366, 2006.

[22] M. R. Ghalenoei, H. Hajimirsadeghi, C. Lucas. Discrete invasive weed optimization algorithm: Application to cooperative multiple task assignment of UAVs. In *Proceedings of the 28h Chinese Control Conference on Decision and Control*, IEEE, Shanghai, China, pp. 1665–1670, 2009.

[23] H. Madivada, C. S. P. Rao. An invasive weed optimization (IWO) approach for multi-objective job shop scheduling problems (JSSPs). *International Journal of Mechanical Engineering and Technology (IJMET)*, vol. 3, no. 3, pp. 627–637, 2012.

[24] Y. Y. Chai, L. M. Jia, Z. D. Zhang. Mamdani model based adaptive neural fuzzy inference system and its application. *International Journal of Computational Intelligence*, vol. 5, no. 1, pp. 22–29, 2009.

[25] A. Hamam, N. D. Georganas. A comparison of Mamdani and Sugeno fuzzy inference systems for evaluating the quality of experience of hapto-audio-visual applications. In *Proceedings of the International Workshop on Haptic Audio Visual Environments and Games*, IEEE, Ottawa, Canada, pp. 87–92, 2008.

[26] H. Kamil. Intelligent Model-based Control of Complex Three-link Mechanisms, Ph. D. dissertation, Cardiff University, UK, 2015.

Hafizul Azizi Ismail received the B. Eng. (Hons) degree in mechatronics engineering from the International Islamic University of Malaysia (IIUM) in 2006, and the M. Eng. degree from Universiti Teknologi Malaysia (UTM) in 2010. Upon graduation he worked as a production engineer in Denso Malaysia Sendirian Berhad before working as a lecturer in German-Malaysian Institute in 2009.

His research interests include artificial intelligence, neural networks, robotics, mechatronics, image processing, optimistion and control engineering.

E-mail: hafizul.azizi@gmail.com (Corresponding author)
ORCID iD: 0000-0002-9594-3700

Michael S. Packianather received the B. Sc. (Hons) degree in electrical and electronic engineering, the M. Sc. and Ph. D. degrees in artificial intelligence from the University of Wales Cardiff (now Cardiff University), UK in 1991, 1993 and 1997 respectively.

His research interests include intelligent manufacturing systems, robotics, neural networks, pattern recognition, expert systems, fault diagnosis, quality control, signal processing, feature selection, data mining and machine learning, optimisation methods, bio-informatics, medical engineering, design of experiments and micro/nano technologies.

E-mail: Packianatherms@cardiff.ac.uk

Roger I. Grosvenor received the B. Eng. (Tech) degree in mechanical engineering from UWIST (now Cardiff University), UK in 1978. He then received the M. Sc. degree in systems engineering in 1984 and the Ph. D. degree in process measurements in 1995, both from Cardiff University, UK. He is a reader and a Year 3 Tutor in mechanical, integrated and medical engineering at the Cardiff School of Engineering.

His research interests include embedded condition monitoring, machine and process monitoring, fault diagnostics & prognostics, data analysis using excel and/or Matlab and signal capture/signal processing.

E-mail: Grosvenor@cardiff.ac.uk